Celestial Mechanics and Dynamical Astronomy (2018) 130:70
https://doi.org/10.1007/s10569-018-9867-z

ORIGINAL ARTICLE

Preliminary orbits with line-of-sight correction for LEO satellites observed with radar

H. Ma[1] · G. Baù[1] · D. Bracali Cioci[2] · G. F. Gronchi[1]

Received: 17 March 2018 / Revised: 6 August 2018 / Accepted: 29 September 2018 /
Published online: 12 October 2018

Abstract
We propose a method to account for the Earth oblateness effect in preliminary orbit determination of satellites in low orbits with radar observations. This method is an improvement of the one described in Gronchi et al. (Mon Not R Astron Soc 451(2):1883–1891, 2015b), which uses a pure Keplerian dynamical model. Since the effect of the Earth oblateness is strong at low altitudes, its inclusion in the model can sensibly improve the initial orbit, giving a better starting guess for differential corrections and increasing the chances to obtain their convergence. The input set consists of two tracks of radar observations, each one composed of at least four observations taken during the same pass of the satellite. A single observation gives the topocentric position of the satellite, where the range is very accurate, while the line-of-sight direction is poorly determined. From these data, we can compute by a polynomial fit the values of the range and range rate at the mean epochs of the two tracks. In order to obtain a preliminary orbit, we wish to compute the angular velocity, which is the rate of change of the line of sight. In the same spirit of Gronchi et al. (Mon Not R Astron Soc 451(2):1883–1891, 2015b), we also wish to correct the values of the angular measurements, so that they fit the selected dynamical model if the same holds for the radial distance and velocity. The selected model is a perturbed Keplerian dynamics, where the only perturbation included is the secular effect of the J_2 term of the geopotential.

Keywords IOD methods · LEO objects · Earth oblateness

✉ G. Baù
giulio.bau@unipi.it

H. Ma
helenema.pro@gmail.com

D. Bracali Cioci
bracalicioci@spacedys.com

G. F. Gronchi
gronchi@dm.unipi.it

[1] Department of Mathematics, Largo Pontecorvo 5, 56127 Pisa, Italy

[2] Space Dynamics Services s.r.l., Via M. Giuntini 63, 56023 Navacchio, Italy

1 Introduction

The growth in the number of space debris orbiting the Earth has increased the interest for the studies of new orbit computation methods, for example Farnocchia et al. (2010), Gronchi et al. (2015a), and of the dynamical properties of Earth satellites, for example Celletti and Galeş (2018), Daquin et al. (2016), Rosengren and Scheeres (2013). Correlating short arcs of observations that belong to the same object and initial orbit determination (IOD) are of crucial importance for surveillance of the current population of space debris. In the case of optical measurements, this problem has been addressed by many authors using different techniques (see, e.g., Siminski et al. 2014 and references therein). On the other hand, only a few methods have been proposed for the case of radar observations (Vananti et al. 2017). In this paper, we investigate an IOD method that is conceived to compute orbits of Earth satellites at low altitudes (LEO) with radar observations.

Let us assume that each radar measurement at epoch t is composed of a precise value of the range ρ (with standard deviation in the order of meters) and poorly determined values of the topocentric right ascension α and declination δ (with standard deviation for example of 0.2 degrees). The available data are radar tracks of the form

$$(t_i, \rho_i, \alpha_i, \delta_i), \qquad i = 1, \ldots, m, \tag{1}$$

where $\Delta t = t_{i+1} - t_i$ is usually a few seconds and $m \geq 4$. Given a radar track, we can derive the vector

$$(\bar{t}, \bar{\alpha}, \bar{\delta}, \rho, \dot{\rho}), \tag{2}$$

where $\bar{\alpha}, \bar{\delta}$ are the mean values while $\rho, \dot{\rho}$ can be obtained through a cubic fit because the measurements of the range are more precise.

We describe the osculating two-body orbit of the satellite by spherical coordinates (also known as *attributable* coordinates)

$$\mathscr{E}_{\text{att}} = (\alpha, \delta, \dot{\alpha}, \dot{\delta}, \rho, \dot{\rho}). \tag{3}$$

Therefore, given the data in (2), to compute an orbit, we need the values of $\dot{\alpha}, \dot{\delta}$, which are the unknowns of our orbit determination problem. We want to correlate two radar attributables at two different epochs corrected for the aberration of light,

$$\tilde{t}_1 = \bar{t}_1 - \rho_1/c, \quad \tilde{t}_2 = \bar{t}_2 - \rho_2/c, \tag{4}$$

where c is the speed of light, to determine the values of $\dot{\alpha}_1, \dot{\alpha}_2, \dot{\delta}_1, \dot{\delta}_2$ and compute a preliminary orbit (see Milani and Gronchi 2010).

Assuming that the motion is Keplerian, Taff and Hall (1977) and more recently Farnocchia et al. (2010) proposed to use the conservation of the angular momentum vector and energy to write a polynomial system which is quadratic in the unknowns. Gronchi et al. (2015b) have recently improved this method by allowing for the correction of the values of $\bar{\alpha}, \bar{\delta}$. For this purpose, they introduce the quantities $\Delta\alpha, \Delta\delta$, which are unknown small deviations from the mean values $\bar{\alpha}, \bar{\delta}$:

$$\alpha = \bar{\alpha} + \Delta\alpha, \qquad \delta = \bar{\delta} + \Delta\delta. \tag{5}$$

The deviations $\Delta\alpha, \Delta\delta$ are called *infinitesimal angles*. Moreover, in place of the unknowns $\dot{\alpha}, \dot{\delta}$ they use the variables

$$\xi = \rho\dot{\alpha}\cos\delta, \qquad \zeta = \rho\dot{\delta}, \tag{6}$$

which are the components of the topocentric velocity of the satellite orthogonal to the line of sight. The orbit at time $\bar{t} - \rho/c$ is completely determined by the *modified attributable* coordinates

$$\mathscr{E}^*_{\rm att} = (\bar{\alpha} + \Delta\alpha, \bar{\delta} + \Delta\delta, \xi, \zeta, \rho, \dot{\rho}). \tag{7}$$

We extend the algorithm introduced in Gronchi et al. (2015b), where a two-body approximation is employed, by considering the secular effect of the J_2 term of the geopotential in the dynamical model. The Earth oblateness has been already considered by Farnocchia et al. (2010) for the computation of preliminary orbits but without introducing corrections to the angles. Their IOD method is iterative, and at each iteration, the problem has the same algebraic structure as the unperturbed one.

We want to determine the values of the eight unknowns $(\Delta\alpha_1, \Delta\delta_1, \xi_1, \zeta_1)$ and $(\Delta\alpha_2, \Delta\delta_2, \xi_2, \zeta_2)$ at $\tilde{t}_1, \tilde{t}_2$ from the input dataset:

$$(\bar{t}_1, \bar{\alpha}_1, \bar{\delta}_1, \rho_1, \dot{\rho}_1), \quad (\bar{t}_2, \bar{\alpha}_2, \bar{\delta}_2, \rho_2, \dot{\rho}_2), \tag{8}$$

using the Keplerian integrals evolution, the equations of motion projected onto the line of sight and a suitable version of Lambert's equation.

2 Notation

Let us denote by $\mathbf{e}^\rho$ the unit vector corresponding to the line of sight, and by $\mathbf{q}$ the geocentric position of the observer. Then, the geocentric position of the observed body is

$$\mathbf{r} = \mathbf{q} + \rho\mathbf{e}^\rho, \tag{9}$$

where ρ is the range. Using as angular coordinates the topocentric right ascension α and declination δ in an equatorial reference frame (e.g., J2000), we have

$$\mathbf{e}^\rho = (\cos\delta\cos\alpha, \cos\delta\sin\alpha, \sin\delta)^{\rm T}. \tag{10}$$

We introduce the unit vectors

$$\mathbf{e}^\alpha = (-\sin\alpha, \cos\alpha, 0)^{\rm T}, \tag{11}$$

$$\mathbf{e}^\delta = (-\sin\delta\cos\alpha, -\sin\delta\sin\alpha, \cos\delta)^{\rm T}. \tag{12}$$

The set $\{\mathbf{e}^\rho, \mathbf{e}^\alpha, \mathbf{e}^\delta\}$ is an orthonormal system. Denoting by $\dot{\mathbf{r}}$ the geocentric velocity of the satellite, we have

$$\dot{\mathbf{r}} = \xi\mathbf{e}^\alpha + \zeta\mathbf{e}^\delta + (\dot{\rho}\mathbf{e}^\rho + \dot{\mathbf{q}}). \tag{13}$$

We will use the following different sets of coordinates for the orbits:

$$\mathscr{E}_{\rm kep} = (a, e, I, \Omega, \omega, \ell), \tag{14}$$

$$\mathscr{E}_{\rm car} = (x, y, z, \dot{x}, \dot{y}, \dot{z}), \tag{15}$$

$$\mathscr{E}_{\rm att} = (\alpha, \delta, \dot{\alpha}, \dot{\delta}, \rho, \dot{\rho}), \tag{16}$$

$$\mathscr{E}^*_{\rm att} = (\bar{\alpha} + \Delta\alpha, \bar{\delta} + \Delta\delta, \xi, \zeta, \rho, \dot{\rho}) \tag{17}$$

that are, respectively, Keplerian, Cartesian, attributable and modified attributable coordinates. Note that the Keplerian elements in (14) have their usual meaning and ℓ denotes the mean anomaly.

We also consider the coordinate changes

$$\mathscr{E}_{\text{kep}} \xrightarrow{\phi_1} \mathscr{E}_{\text{car}}, \qquad \mathscr{E}_{\text{car}} \xrightarrow{\phi_2} \mathscr{E}_{\text{att}}, \qquad \mathscr{E}_{\text{att}} \xrightarrow{\phi_3} \mathscr{E}^*_{\text{att}}, \tag{18}$$

and the composite transformation

$$\Phi = \phi_3 \circ \phi_2 \circ \phi_1 \tag{19}$$

from $\mathscr{E}_{\text{kep}}$ to $\mathscr{E}^*_{\text{att}}$.

3 The equations of motion

Let us consider Newton's equation

$$\ddot{\mathbf{r}} = \nabla U(\mathbf{r}), \tag{20}$$

for the motion of a point mass in the Earth gravity field where the force function U is truncated at the J_2-term that is

$$U(\mathbf{r}) = \frac{\mu}{r}\Big[1 - J_2\Big(\frac{R_\oplus}{r}\Big)^2 P_2(\sin\delta)\Big]. \tag{21}$$

Here, $r = |\mathbf{r}|$ is the geocentric distance, $R_\oplus$ is the equatorial radius of the Earth and P_2 is the Legendre polynomial of second degree

$$P_2(\sin\delta) = \frac{3}{2}\sin^2\delta - \frac{1}{2} = \frac{3}{2}\frac{z^2}{r^2} - \frac{1}{2}. \tag{22}$$

The problem defined by Eq. (20) is non-integrable (see Celletti and Negrini 1981). If we average out the short period term in (20), we obtain an integrable system (see Roy 2004) given by

$$\begin{cases} \dot{a} = 0, \\ \dot{e} = 0, \\ \dot{I} = 0, \\ \dot{\Omega} = -\dfrac{3}{2}J_2\dfrac{R_\oplus^2}{p^2}\tilde{n}\cos I, \\ \dot{\omega} = \dfrac{3}{4}J_2\dfrac{R_\oplus^2}{p^2}\tilde{n}(4 - 5\sin^2 I), \\ \dot{\ell} = \tilde{n} = n\Big[1 + \dfrac{3}{2}J_2\dfrac{R_\oplus^2}{p^2}\Big(1 - \dfrac{3}{2}\sin^2 I\Big)\sqrt{1-e^2}\Big], \end{cases} \tag{23}$$

with $p = a(1-e^2)$ the parameter of the two-body trajectory and $n = \sqrt{\mu/a^3}$ the mean motion. Note that in the dynamics defined by (23), the elements a, e, I remain constant while the ascending node Ω, the argument of perigee ω and the mean anomaly ℓ change uniformly with time. Equation (23) can be written shortly as

$$\dot{\mathscr{E}}_{\text{kep}} = \mathbf{X}_{\text{kep}}(\mathscr{E}_{\text{kep}}). \tag{24}$$

In the following, we shall assume that the observed body is moving according to the integrable dynamics defined by Eqs. (23), (24), and we shall call oblateness effect (or J_2 effect) the deviation from the pure Keplerian motion which is defined by these equations.

To solve our problem, we express the equations of motion in terms of the coordinates $\mathscr{E}^*_{\rm att}$. First, we write Eq. (24) in Cartesian coordinates $\mathscr{E}_{\rm car} = (\mathbf{r}, \dot{\mathbf{r}})$. We obtain

$$\dot{\mathscr{E}}_{\rm car} = \mathbf{Y}(\mathscr{E}_{\rm car}), \tag{25}$$

where

$$\mathbf{Y} = \left(\frac{\partial \phi_1}{\partial \mathscr{E}_{\rm kep}} \mathbf{X}_{\rm kep}\right) \circ \phi_1^{-1} \tag{26}$$

is the transformed vector field. From the expression above, we obtain the acceleration $\ddot{\mathbf{r}}$ as a function of $\mathscr{E}_{\rm car}$ along the solutions of (25):

$$\ddot{\mathbf{r}} = \left(\frac{\partial \dot{\mathbf{r}}}{\partial \mathscr{E}_{\rm kep}} \mathbf{X}_{\rm kep}\right) \circ \phi_1^{-1} =: \tilde{\mathbf{y}}(\mathbf{r}, \dot{\mathbf{r}}). \tag{27}$$

As done in Gronchi et al. (2015b) for the pure Keplerian dynamics, we project the perturbed equation of motion (27) along the line of sight $\mathbf{e}^\rho$ and obtain the equation

$$\mathcal{K} = 0, \tag{28}$$

with

$$\mathcal{K} = (\ddot{\mathbf{r}} - \tilde{\mathbf{y}}) \cdot \mathbf{e}^\rho = \ddot{\rho} - \rho\eta^2 + \ddot{\mathbf{q}} \cdot \mathbf{e}^\rho - \tilde{\mathbf{y}} \cdot \mathbf{e}^\rho, \tag{29}$$

where $\eta = \sqrt{\dot{\alpha}^2 \cos^2 \delta + \dot{\delta}^2}$ is the proper motion.

Equation (29) can be expressed as a function of the unknown variables $(\Delta\alpha, \Delta\delta, \xi, \zeta)$ using the expressions of $\mathbf{r}, \dot{\mathbf{r}}$ given in (9), (13).

4 The J_2 effect on the two-body integrals

We recall the expressions of the conserved quantities in the Keplerian dynamics, i.e., the angular momentum $\mathbf{c}$, the energy $\mathcal{E}$ and the Laplace–Lenz vector $\mathbf{L}$, as a function of $\mathbf{r}, \dot{\mathbf{r}}$. These quantities can be read as functions of the attributable coordinates $\mathscr{E}_{\rm att}$ using (9), (13) and

$$|\dot{\mathbf{r}}|^2 = \xi^2 + \zeta^2 + 2\dot{\mathbf{q}} \cdot \mathbf{e}^\alpha \xi + 2\dot{\mathbf{q}} \cdot \mathbf{e}^\delta \zeta + |\dot{\rho}\mathbf{e}^\rho + \dot{\mathbf{q}}|^2, \tag{30}$$

$$\dot{\mathbf{r}} \cdot \mathbf{r} = \mathbf{q} \cdot \mathbf{e}^\alpha \xi + \mathbf{q} \cdot \mathbf{e}^\delta \zeta + (\dot{\rho}\mathbf{e}^\rho + \dot{\mathbf{q}}) \cdot \mathbf{r}. \tag{31}$$

We have

$$\mathbf{c} = \mathbf{A}\xi + \mathbf{B}\zeta + \mathbf{C}, \tag{32}$$

$$\mathcal{E} = \frac{1}{2}|\dot{\mathbf{r}}|^2 - \frac{\mu}{|\mathbf{r}|}, \tag{33}$$

$$\mu\mathbf{L} = \dot{\mathbf{r}} \times \mathbf{c} - \mu\frac{\mathbf{r}}{|\mathbf{r}|} = \left(|\dot{\mathbf{r}}|^2 - \frac{\mu}{|\mathbf{r}|}\right)\mathbf{r} - (\dot{\mathbf{r}} \cdot \mathbf{r})\dot{\mathbf{r}}, \tag{34}$$

where

$$\mathbf{A} = \mathbf{r} \times \mathbf{e}^\alpha, \quad \mathbf{B} = \mathbf{r} \times \mathbf{e}^\delta, \quad \mathbf{C} = \mathbf{r} \times \dot{\mathbf{q}} + \dot{\rho}\,\mathbf{q} \times \mathbf{e}^\rho. \tag{35}$$

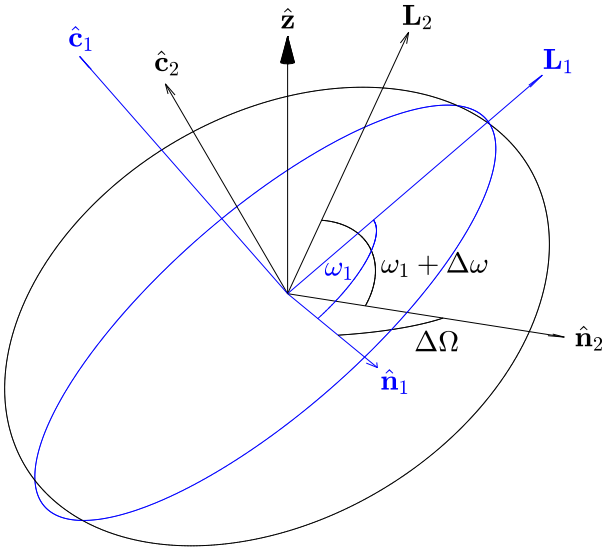

Fig. 1 According to the secular effect of the J_2 term [see Eq. (23)], the shape of the conic and its inclination remain unchanged between two epochs $\tilde{t}_1, \tilde{t}_2$. The directions of the angular momentum ($\hat{\mathbf{c}}$), line of nodes ($\hat{\mathbf{n}}$) and Laplace–Lenz vector ($\mathbf{L}$), by contrast, are rotated due to the secular variations $\Delta\Omega$, $\Delta\omega$ accumulated by Ω, ω during the time interval $\tilde{t}_2 - \tilde{t}_1$

Including the J_2 effect in the dynamics, the angular momentum and the Laplace–Lenz vectors are not conserved anymore. However, the following relations hold:

$$R_c \mathbf{c}_1 = \mathbf{c}_2, \tag{36}$$

$$\mathcal{E}_1 = \mathcal{E}_2, \tag{37}$$

$$R_L \mathbf{L}_1 = \mathbf{L}_2, \tag{38}$$

where

$$R_c = R_{\hat{\mathbf{z}}}(\Delta\Omega), \qquad R_L = R_{\hat{\mathbf{c}}_2}(\omega_1 + \Delta\omega)\, R_{\hat{\mathbf{z}}}(\Delta\Omega)\, R_{\hat{\mathbf{c}}_1}(-\omega_1). \tag{39}$$

Here, we denote by $R_{\hat{\mathbf{v}}}(\varphi)$ the rotation matrix defined by the rotation of an angle φ around the axis of the unit vector $\hat{\mathbf{v}}$. Then, the unit vectors $\hat{\mathbf{z}}$, $\hat{\mathbf{c}}_i$, $i = 1, 2$, are given by

$$\hat{\mathbf{z}} = (0,\ 0,\ 1)^{\mathrm{T}}, \tag{40}$$

$$\hat{\mathbf{c}}_i = (\sin\Omega_i \sin I_i,\ -\cos\Omega_i \sin I_i,\ \cos I_i)^{\mathrm{T}}. \tag{41}$$

Moreover, using Eq. (23), the angular variations $\Delta\Omega$ and $\Delta\omega$ are obtained as

$$\Delta\Omega = \dot{\Omega}_1(\tilde{t}_2 - \tilde{t}_1), \qquad \Delta\omega = \dot{\omega}_1(\tilde{t}_2 - \tilde{t}_1), \tag{42}$$

where $\tilde{t}_1, \tilde{t}_2$ are the epochs corrected by aberration. We display the J_2 effect on the two-body integrals in Fig. 1.

Remark 1 We can also write

$$\Delta\Omega = \Omega_2 - \Omega_1, \qquad \Delta\omega = \omega_2 - \omega_1, \tag{43}$$

and

$$R_L = R_2 R_1^{\mathrm{T}}, \tag{44}$$

with

$$R_i = R_{\hat{\mathbf{c}}_i}(\omega_i)\, R_{\hat{\mathbf{z}}}(\Omega_i), \qquad i = 1, 2. \tag{45}$$

5 Lambert's theorem with the J_2 effect

Let us denote by $\mathcal{L}$ the expression defining Lambert's equation. In the dynamics given by (23), the mean motion evolves linearly; thus, Lambert's equation can be written as

$$\mathcal{L} = \tilde{n}(\tilde{t}_1 - \tilde{t}_2) + (\beta - \sin\beta) - (\gamma - \sin\gamma) + 2k\pi = 0, \tag{46}$$

with $\tilde{n}$ given by the last equation in (23). Moreover, $k \in \mathbb{N}$ is the number of revolutions in the time interval $[\tilde{t}_1, \tilde{t}_2]$. The angles β, γ are defined by

$$\sin^2\frac{\beta}{2} = \frac{r_1 + r_2 + d_L}{4a}, \qquad \sin^2\frac{\gamma}{2} = \frac{r_1 + r_2 - d_L}{4a}, \tag{47}$$

where $0 \le \beta - \gamma \le 2\pi$ and r_1, r_2 are the distances from the center of force. In (47), the distance

$$d_L = |\tilde{R}\mathbf{r}_1 - \mathbf{r}_2| \tag{48}$$

is the length of the chord joining the two positions of the body at epochs $\tilde{t}_1$, $\tilde{t}_2$ after rotating the osculating ellipse at epoch $\tilde{t}_1$ so that it overlaps with the osculating ellipse at epoch $\tilde{t}_2$. The rotation $\tilde{R}$ is given explicitly by

$$\tilde{R} = \tilde{R}_2\tilde{R}_1^{\mathrm{T}}, \tag{49}$$

with $\tilde{R}_1$ and $\tilde{R}_2$ the transformations from the selected equatorial reference frame to the orbital reference frame at the epochs $\tilde{t}_1$ and $\tilde{t}_2$, respectively:

$$\tilde{R}_1 = R_{\hat{\mathbf{c}}_1}(\omega_1)\, R_{\hat{\mathbf{n}}_1}(I_1)\, R_{\hat{\mathbf{z}}}(\Omega_1), \tag{50}$$

$$\tilde{R}_2 = R_{\hat{\mathbf{c}}_2}(\omega_1 + \Delta\omega)\, R_{\hat{\mathbf{n}}_2}(I_2)\, R_{\hat{\mathbf{z}}}(\Omega_1 + \Delta\Omega), \tag{51}$$

where

$$\hat{\mathbf{n}}_i = (\cos\Omega_i,\ \sin\Omega_i,\ 0)^{\mathrm{T}}, \quad i = 1, 2, \tag{52}$$

are the directions of the lines of nodes. For a fixed number of revolutions k, we have four different choices for the pairs (β, γ) (see Appendix A1 in Gronchi et al. 2015b, for the details).

6 Linkage

We wish to link two sets of radar data of the form (2), with mean epochs $\bar{t}_i$, $i = 1, 2$, and compute one (or more) preliminary orbits. In the following, we use labels 1, 2 for the quantities introduced in the previous sections, according to the epoch. Moreover, let us define $\boldsymbol{\nu}_2 = \mathbf{e}_2^{\rho} \times \mathbf{q}_2$.

Taking into account the J_2 effect, we consider the following system:

$$(R_c\mathbf{c}_1 - \mathbf{c}_2,\ \mathcal{E}_1 - \mathcal{E}_2,\ \mathcal{K}_1,\ \mathcal{K}_2,\ (R_L\mathbf{L}_1 - \mathbf{L}_2)\cdot\boldsymbol{\nu}_2,\ \mathcal{L}) = \mathbf{0} \tag{53}$$

of eight equations in the eight unknowns $(\mathbf{X},\ \boldsymbol{\Delta})$, with

$$\mathbf{X} = (\xi_1,\ \zeta_1,\ \xi_2,\ \zeta_2), \qquad \boldsymbol{\Delta} = (\Delta\alpha_1,\ \Delta\delta_1,\ \Delta\alpha_2,\ \Delta\delta_2). \tag{54}$$

Note that the unknowns are divided into two sets so that $\boldsymbol{\Delta}$ is the vector of infinitesimal angles.

In Gronchi et al. (2015a, b), because the motion is assumed Keplerian, $\mathbf{X}(\boldsymbol{\Delta})$ is obtained explicitly from the conservation of the angular momentum and energy. The remaining equations are solved for $\boldsymbol{\Delta}$ using an iterative scheme. In our method, we also separate system (53) into two subsystems which can be solved by a double-iterative scheme. We search for solutions of equation

$$\mathcal{G}(\boldsymbol{\Delta}) = \mathbf{G}(\mathbf{X}(\boldsymbol{\Delta}), \boldsymbol{\Delta}) = \mathbf{0}, \tag{55}$$

where

$$\mathbf{G} = (\mathcal{K}_1,\ \mathcal{K}_2,\ (R_L\mathbf{L}_1 - \mathbf{L}_2)\cdot \boldsymbol{v}_2,\ \mathcal{L}) \tag{56}$$

and $\mathbf{X}(\boldsymbol{\Delta})$ is implicitly defined by the relation

$$\mathbf{J}(\mathbf{X}, \boldsymbol{\Delta}) = \mathbf{0}, \tag{57}$$

where

$$\mathbf{J} = (R_c\mathbf{c}_1 - \mathbf{c}_2,\ \mathcal{E}_1 - \mathcal{E}_2). \tag{58}$$

Newton–Raphson method is used to compute $\boldsymbol{\Delta}$ from the iterative formula

$$\boldsymbol{\Delta}_{h+1} = \boldsymbol{\Delta}_h - \left[\frac{\partial \mathcal{G}}{\partial \boldsymbol{\Delta}}(\boldsymbol{\Delta}_h)\right]^{-1}\mathcal{G}(\boldsymbol{\Delta}_h), \qquad \boldsymbol{\Delta}_0 = \mathbf{0}. \tag{59}$$

Here, taking advantage of the assumed smallness of the solutions $\boldsymbol{\Delta}$, we consider $\boldsymbol{\Delta} = \mathbf{0}$ as starting guess. At each iteration for $\boldsymbol{\Delta}$, we apply the Newton–Raphson method to obtain $\mathbf{X}(\boldsymbol{\Delta})$ from system (57). Precisely, for $\boldsymbol{\Delta} = \boldsymbol{\Delta}_h$, we compute $\mathbf{X}^{(h)} = \mathbf{X}(\boldsymbol{\Delta}_h)$ from the iterative formula

$$\mathbf{X}_{j+1} = \mathbf{X}_j - \left[\frac{\partial \mathcal{J}}{\partial \mathbf{X}}(\mathbf{X}_j)\right]^{-1}\mathcal{J}(\mathbf{X}_j), \tag{60}$$

where

$$\mathcal{J}(\mathbf{X}) = \mathbf{J}(\mathbf{X}, \boldsymbol{\Delta}_h). \tag{61}$$

For $h = 0$ the starting guess $\mathbf{X}_0$ is computed from the interpolated values of $\delta, \dot{\alpha}, \dot{\delta}, \rho$ through Equations (6), while for $h > 0$ we set $\mathbf{X}_0 = \mathbf{X}^{(h-1)}$.

Remark 2 Equation (57) is not polynomial in $\mathbf{X}$, unlike the corresponding equations in Gronchi et al. (2015b).

7 Computing X, Δ

The algorithm to compute the vectors $\mathbf{X}$, $\boldsymbol{\Delta}$ that satisfy Eq. (53) consists of two nested Newton–Raphson methods. Starting from $\boldsymbol{\Delta}_0 = \mathbf{0}$, we determine the vector $\mathbf{X}^{(0)}$ such that $\mathbf{J}(\mathbf{X}^{(0)}, \boldsymbol{\Delta}_0) = \mathbf{0}$, by applying the Newton–Raphson formula (60), wherein $\mathcal{J}(\mathbf{X}) = \mathbf{J}(\mathbf{X}, \boldsymbol{\Delta}_0)$. Then, after computing the number of revolutions k required in Lambert's equation (46), by

$$k = \left\lfloor \frac{n(\tilde{t}_2 - \tilde{t}_1)}{2\pi} \right\rfloor, \tag{62}$$

where n is the mean motion and $\lfloor x \rfloor$ denotes the integer part of x, we make the first iteration of the outer Newton–Raphson method through Eq. (59), wherein $\mathcal{G}(\boldsymbol{\Delta}_0) = \mathbf{G}(\mathbf{X}^{(0)}, \boldsymbol{\Delta}_0)$.

The iterations in $\boldsymbol{\Delta}$ are carried out until for some $h \geq 1$ the magnitude of the difference $\boldsymbol{\Delta}_h - \boldsymbol{\Delta}_{h-1}$ is smaller than a suitable tolerance. Finally, $\mathbf{X}^{(h)}$ is obtained by the iterative formula (60), and the solution of (53) is given by the pair of vectors $\mathbf{X}^{(h)}$, $\boldsymbol{\Delta}_h$.

In Eq. (55), the components of the vector $\mathbf{G}(\mathbf{X}, \boldsymbol{\Delta})$ are similar to the ones of the corresponding vector in Gronchi et al. (2015b). However, the following differences occur:

(i) in place of the angular momentum conservation law, we have Eq. (36);
(ii) in $\mathcal{K}$ at epochs $\tilde{t}_1, \tilde{t}_2$, the term $\tilde{\mathbf{y}} \cdot \mathbf{e}^\rho$ replaces the radial component of the Keplerian force, i.e., $-\mu \mathbf{r} \cdot \mathbf{e}^\rho / |\mathbf{r}|^3$;
(iii) in place of the Laplace–Lenz conservation law, we have Eq. (38);
(iv) in $\mathcal{L}$, the quantity $\tilde{n}$ takes a different expression from the mean motion n, coming from the dynamical model (23). Moreover, the length of the chord is computed in a different way; see (48).

To search for the values of $\boldsymbol{\Delta}$ that solve Eq. (55), we have to compute the first derivatives of $\mathcal{G}(\boldsymbol{\Delta})$ with respect to $\boldsymbol{\Delta}$, appearing in (59), that is

$$\frac{\partial \mathcal{G}}{\partial \boldsymbol{\Delta}}(\boldsymbol{\Delta}_h) = \frac{\partial \mathbf{G}}{\partial \mathbf{X}}(\mathbf{X}^{(h)}, \boldsymbol{\Delta}_h) \frac{\partial \mathbf{X}}{\partial \boldsymbol{\Delta}}(\boldsymbol{\Delta}_h) + \frac{\partial \mathbf{G}}{\partial \boldsymbol{\Delta}}(\mathbf{X}^{(h)}, \boldsymbol{\Delta}_h). \tag{63}$$

From the implicit function theorem applied to Eq. (57), we have

$$\frac{\partial \mathbf{X}}{\partial \boldsymbol{\Delta}}(\boldsymbol{\Delta}) = -\left[\frac{\partial \mathbf{J}}{\partial \mathbf{X}}(\mathbf{X}, \boldsymbol{\Delta})\right]^{-1} \frac{\partial \mathbf{J}}{\partial \boldsymbol{\Delta}}(\mathbf{X}, \boldsymbol{\Delta}). \tag{64}$$

Since these computations are similar to the ones reported in Gronchi et al. (2015b, Sect. 7), we describe below only the differences coming from the adopted dynamical model.

7.1 The derivatives of $R_c\mathbf{c}_1 - \mathbf{c}_2, \mathcal{E}_1 - \mathcal{E}_2$

The derivatives of $R_c\mathbf{c}_1 - \mathbf{c}_2$ with respect to a component x of the vectors $\mathbf{X}$, $\boldsymbol{\Delta}$ can be written as

$$\frac{\partial (R_c\mathbf{c}_1 - \mathbf{c}_2)}{\partial x} = \frac{\partial R_c}{\partial x}\mathbf{c}_1 + R_c \frac{\partial \mathbf{c}_1}{\partial x} - \frac{\partial \mathbf{c}_2}{\partial x}. \tag{65}$$

We have

$$\frac{\partial R_c}{\partial x} = \begin{bmatrix} -\sin\Delta\Omega & -\cos\Delta\Omega & 0 \\ \cos\Delta\Omega & -\sin\Delta\Omega & 0 \\ 0 & 0 & 0 \end{bmatrix} \frac{\partial \Delta\Omega}{\partial x}, \tag{66}$$

where

$$\frac{\partial \Delta\Omega}{\partial x} = \frac{\partial \dot{\Omega}_1}{\partial x}\Delta t, \tag{67}$$

and the expressions of $\frac{\partial \dot{\Omega}_1}{\partial x}$ are reported in "Appendix C".

Considering the angular momentum, we get

$$\frac{\partial \mathbf{c}_i}{\partial \xi_i} = \mathbf{A}_i, \qquad \frac{\partial \mathbf{c}_i}{\partial \zeta_i} = \mathbf{B}_i, \qquad i = 1, 2. \tag{68}$$

The derivatives with respect to $\mathbf{\Delta}$ are computed through the intermediate variables $\mathbf{e}_i^\rho$, $\mathbf{e}_i^\alpha$, $\mathbf{e}_i^\delta$, $i = 1, 2$. After introducing the vector

$$\mathbf{E}_i = \begin{pmatrix} \mathbf{e}_i^\rho \\ \mathbf{e}_i^\alpha \\ \mathbf{e}_i^\delta \end{pmatrix}, \tag{69}$$

we can write

$$\frac{\partial \mathbf{c}_i}{\partial \mathbf{E}_i} = \frac{\partial \mathbf{A}_i}{\partial \mathbf{E}_i}\xi_i + \frac{\partial \mathbf{B}_i}{\partial \mathbf{E}_i}\zeta_i + \frac{\partial \mathbf{C}_i}{\partial \mathbf{E}_i}, \tag{70}$$

with

$$\frac{\partial \mathbf{A}_i}{\partial \mathbf{E}_i} = (O_3,\ S(\mathbf{q}_i),\ \rho_i I_3), \tag{71}$$

$$\frac{\partial \mathbf{B}_i}{\partial \mathbf{E}_i} = (O_3,\ -\rho_i I_3,\ S(\mathbf{q}_i)), \tag{72}$$

$$\frac{\partial \mathbf{C}_i}{\partial \mathbf{E}_i} = (-\rho_i S(\dot{\mathbf{q}}_i) + \dot{\rho}_i S(\mathbf{q}_i),\ O_3,\ O_3), \tag{73}$$

where O_3, I_3 denote the 3×3 zero and identity matrix, respectively. Note that $S(\mathbf{a})$ is the skew-symmetric matrix associated with a vector $\mathbf{a} = (a_1, a_2, a_3)^{\mathrm{T}}$ by

$$S(\mathbf{a})\,\mathbf{y} = \mathbf{a} \times \mathbf{y}, \qquad \forall \mathbf{y} \in \mathbb{R}^3, \tag{74}$$

that is

$$\mathbb{R}^3 \ni \mathbf{a} \mapsto S(\mathbf{a}) \overset{def}{=} \begin{bmatrix} 0 & -a_3 & a_2 \\ a_3 & 0 & -a_1 \\ -a_2 & a_1 & 0 \end{bmatrix}. \tag{75}$$

Concerning the energy, we have[1]

$$\frac{\partial \mathcal{E}_i}{\partial \xi_i} = \xi_i + \dot{\mathbf{q}}_i \cdot \mathbf{e}_i^\alpha, \qquad \frac{\partial \mathcal{E}_i}{\partial \zeta_i} = \zeta_i + \dot{\mathbf{q}}_i \cdot \mathbf{e}_i^\delta, \tag{76}$$

$$\frac{\partial \mathcal{E}_i}{\partial \mathbf{E}_i} = \left(\dot{\rho}_i \dot{\mathbf{q}}_i + \mu \rho_i \frac{\mathbf{q}_i}{r_i^3},\ \xi_i \dot{\mathbf{q}}_i,\ \zeta_i \dot{\mathbf{q}}_i\right). \tag{77}$$

Finally, the derivatives $\frac{\partial \mathbf{E}_i}{\partial(\Delta\alpha_i, \Delta\delta_i)}$, $i = 1, 2$, can be found in Gronchi et al. (2015b, Sect. 7.2).

7.2 The derivatives of $(R_L \mathbf{L_1} - \mathbf{L_2}) \cdot \boldsymbol{v_2}$, $\mathcal{L}$

The derivative of R_L with respect to a component x of the vectors $\mathbf{X}$, $\mathbf{\Delta}$ is obtained from Eq. (44) as

$$\frac{\partial R_L}{\partial x} = \frac{\partial R_2}{\partial x} R_1^{\mathrm{T}} - R_2 R_1^{\mathrm{T}} \frac{\partial R_1}{\partial x} R_1^{\mathrm{T}}, \tag{78}$$

where we have used that R_1 is an orthogonal matrix. A similar expression can be written for $\tilde{R}$ starting from (49). The rotation matrices in (39), (50), (51) are represented by means of Euler–Rodrigues formula (see Gallego and Yezzi 2015)

$$R_{\hat{\mathbf{v}}}(\varphi) = I_3 + \sin\varphi\, S(\hat{\mathbf{v}}) + (1 - \cos\varphi) S^2(\hat{\mathbf{v}}), \tag{79}$$

[1] There is a typo in the equation for $\frac{\partial \mathcal{E}_1}{\partial \mathbf{X}}$ reported in Gronchi et al. (2015b, Sect. 7.1)

where I_3 is the identity matrix and $S(\hat{\mathbf{v}})$ is the skew-symmetric matrix associated with the unit vector $\hat{\mathbf{v}} = (v_1, v_2, v_3)^{\mathrm{T}}$. Then, we have

$$\frac{\partial R_{\hat{\mathbf{v}}}(\varphi)}{\partial x} = \sum_{k=1}^{3} \frac{\partial R_{\hat{\mathbf{v}}}(\varphi)}{\partial v_k} \frac{\partial v_k}{\partial x} + \frac{\partial R_{\hat{\mathbf{v}}}(\varphi)}{\partial \varphi} \frac{\partial \varphi}{\partial x}, \tag{80}$$

where

$$\frac{\partial R_{\hat{\mathbf{v}}}(\varphi)}{\partial v_k} = \sin\varphi \frac{\partial S(\hat{\mathbf{v}})}{\partial v_k} + (1 - \cos\varphi)\Big(\frac{\partial S(\hat{\mathbf{v}})}{\partial v_k} S(\hat{\mathbf{v}}) + S(\hat{\mathbf{v}}) \frac{\partial S(\hat{\mathbf{v}})}{\partial v_k}\Big) \tag{81}$$

and

$$\frac{\partial R_{\hat{\mathbf{v}}}(\varphi)}{\partial \varphi} = \cos\varphi\, S(\hat{\mathbf{v}}) + \sin\varphi\, S^2(\hat{\mathbf{v}}). \tag{82}$$

The derivatives of $\hat{\mathbf{v}}$ are obtained from (41), (52) and using $\frac{\partial \Phi^{-1}}{\partial x}$, which is given in "Appendix B". Note that

$$\frac{\partial \Omega_2}{\partial x} = \frac{\partial \Omega_1}{\partial x} + \frac{\partial \dot{\Omega}_1}{\partial x}(\tilde{t}_2 - \tilde{t}_1), \tag{83}$$

$$\frac{\partial \omega_2}{\partial x} = \frac{\partial \omega_1}{\partial x} + \frac{\partial \dot{\omega}_1}{\partial x}(\tilde{t}_2 - \tilde{t}_1) \tag{84}$$

and $\frac{\partial(\dot{\Omega}_1, \dot{\omega}_1)}{\partial x}$ are reported in "Appendix C".

Regarding Laplace–Lenz conservation law, the derivatives of $\mathbf{L}_1 \cdot \boldsymbol{v}_2, \mathbf{L}_2 \cdot \boldsymbol{v}_2$ are provided in Gronchi et al. (2015b, Sections 7.1, 7.3).

For Lambert's equation, we have

$$\frac{\partial \mathcal{L}}{\partial x} = \frac{\partial \tilde{n}_1}{\partial x}(\tilde{t}_1 - \tilde{t}_2) + \frac{\partial(\beta - \sin\beta)}{\partial x} - \frac{\partial(\gamma - \sin\gamma)}{\partial x}. \tag{85}$$

The derivatives of $\tilde{n}_1$ are computed from (23) as shown in "Appendix C". Moreover,[2]

$$\frac{\partial(\beta - \sin\beta)}{\partial x} = \pm 2\sqrt{\frac{\Gamma_+}{1 - \Gamma_+}} \frac{\partial \Gamma_+}{\partial x}, \tag{86}$$

$$\frac{\partial(\gamma - \sin\gamma)}{\partial x} = \pm 2\sqrt{\frac{\Gamma_-}{1 - \Gamma_-}} \frac{\partial \Gamma_-}{\partial x}, \tag{87}$$

where the positive sign holds for $0 < \beta, \gamma < \pi$. The quantities $\Gamma_\pm = (\Gamma_+, \Gamma_-)$ are defined as in Gronchi et al. (2015b, Sect. 7.1), where d is replaced by d_L, so that

$$\frac{\partial \Gamma_\pm}{\partial \mathbf{X}} = -\frac{r_1 + r_2 \pm d_L}{2\mu} \frac{\partial \mathcal{E}_1}{\partial \mathbf{X}} \mp \frac{\mathcal{E}_1}{2\mu} \frac{\partial d_L}{\partial \mathbf{X}}, \tag{88}$$

$$\frac{\partial \Gamma_\pm}{\partial \boldsymbol{\Delta}} = -\frac{r_1 + r_2 \pm d_L}{2\mu} \frac{\partial \mathcal{E}_1}{\partial \boldsymbol{\Delta}} - \frac{\mathcal{E}_1}{2\mu} \frac{\partial (r_1 + r_2 \pm d_L)}{\partial \boldsymbol{\Delta}}, \tag{89}$$

where

$$\frac{\partial r_i}{\partial(\Delta\alpha_i, \Delta\delta_i)} = \frac{\rho_i}{r_i}(\cos\delta_i \mathbf{q}_i \cdot \mathbf{e}_i^\alpha,\ \mathbf{q}_i \cdot \mathbf{e}_i^\delta), \tag{90}$$

$$\frac{\partial d_L}{\partial x} = \frac{1}{d_L}\Big(\frac{\partial \tilde{R}}{\partial x}\mathbf{r}_1 + \tilde{R}\frac{\partial \mathbf{r}_1}{\partial x} - \frac{\partial \mathbf{r}_2}{\partial x}\Big) \cdot (\tilde{R}\mathbf{r}_1 - \mathbf{r}_2), \tag{91}$$

[2] There is a typo in the corresponding formulae in Gronchi et al. (2015b, Sections 7.1, 7.3).

and

$$\frac{\partial \mathbf{r}_i}{\partial(\Delta\alpha_i, \Delta\delta_i)} = \rho_i(\cos\delta_i \mathbf{e}_i^{\alpha}, \mathbf{e}_i^{\delta}). \tag{92}$$

7.3 The derivatives of $\mathcal{K}_1, \mathcal{K}_2$

The value of $\ddot{\rho}$ is required in the equation of motion (94) at the two epochs $\tilde{t}_1, \tilde{t}_2$. The quantity $\ddot{\rho}$ is regarded as a constant whose value is updated by means of Eq. (94) at each iteration of Newton–Raphson method for computing $\mathbf{\Delta}$. Note that in this way the values taken by $\mathcal{K}_1$, $\mathcal{K}_2$ are always identically 0.

Since $\mathcal{K}$ depends on quantities that are referred to the same epoch, we will drop the subscript i.

We need to compute:

$$\frac{\partial \mathcal{K}}{\partial \mathscr{E}^*_{\rm att}} = \frac{\partial(\ddot{\mathbf{r}} \cdot \mathbf{e}^{\rho})}{\partial \mathscr{E}^*_{\rm att}} - \frac{\partial(\tilde{\mathbf{y}} \cdot \mathbf{e}^{\rho})}{\partial \mathscr{E}^*_{\rm att}}. \tag{93}$$

From the equation

$$\ddot{\mathbf{r}} \cdot \mathbf{e}^{\rho} = \ddot{\rho} - \rho\eta^2 + \ddot{\mathbf{q}} \cdot \mathbf{e}^{\rho}, \tag{94}$$

we obtain

$$\frac{\partial(\ddot{\mathbf{r}} \cdot \mathbf{e}^{\rho})}{\partial \mathscr{E}^*_{\rm att}} = \left(\ddot{\mathbf{q}} \cdot \frac{\partial \mathbf{e}^{\rho}}{\partial \Delta\alpha}, \ddot{\mathbf{q}} \cdot \frac{\partial \mathbf{e}^{\rho}}{\partial \Delta\delta}, -\frac{2\xi}{\rho}, -\frac{2\zeta}{\rho}, \eta^2, 0\right), \tag{95}$$

with

$$\frac{\partial \mathbf{e}^{\rho}}{\partial \Delta\alpha} = \frac{\partial \mathbf{e}^{\rho}}{\partial \alpha} = \mathbf{e}^{\alpha}\cos\delta, \qquad \frac{\partial \mathbf{e}^{\rho}}{\partial \Delta\delta} = \frac{\partial \mathbf{e}^{\rho}}{\partial \delta} = \mathbf{e}^{\delta}. \tag{96}$$

In (96), we made a little abuse of notation: $\mathbf{e}^{\rho}$ stands for both a function of (α, δ) and $(\Delta\alpha, \Delta\delta)$.

Then, we introduce $\mathbf{y}^*$, i.e., the vector $\tilde{\mathbf{y}}$ (see 27) as a function of the coordinates $\mathscr{E}^*_{\rm att}$:

$$\mathbf{y}^* = \tilde{\mathbf{y}} \circ \phi_2^{-1} \circ \phi_3^{-1} = \left(\frac{\partial \dot{\mathbf{r}}}{\partial \mathscr{E}^*_{\rm att}} \mathbf{X}_{\rm kep}\right) \circ \Phi^{-1}. \tag{97}$$

Denoting by $x_{(k)}$ the k-th component of x (where x can be here either a vector or a map), we can write

$$\mathbf{y}^*_{(k)} = \left(\frac{\partial \dot{\mathbf{r}}_{(k)}}{\partial \mathscr{E}_{\rm kep}} \mathbf{X}_{\rm kep}\right) \circ \Phi^{-1}, \quad k = 1, 2, 3. \tag{98}$$

Their derivatives are given by

$$\frac{\partial \mathbf{y}^*_{(k)}}{\partial \mathscr{E}^*_{\rm att}} = \left[\frac{\partial}{\partial \mathscr{E}_{\rm kep}}\left(\frac{\partial \dot{\mathbf{r}}_{(k)}}{\partial \mathscr{E}_{\rm kep}} \mathbf{X}_{\rm kep}\right)\right] \circ \Phi^{-1} \frac{\partial \Phi^{-1}}{\partial \mathscr{E}^*_{\rm att}}, \tag{99}$$

where

$$\frac{\partial}{\partial \mathscr{E}_{\rm kep}}\left(\frac{\partial \dot{\mathbf{r}}_{(k)}}{\partial \mathscr{E}_{\rm kep}} \mathbf{X}_{\rm kep}\right) = \frac{\partial^2 \dot{\mathbf{r}}_{(k)}}{\partial \mathscr{E}^2_{\rm kep}} \mathbf{X}_{\rm kep} + \frac{\partial \dot{\mathbf{r}}_{(k)}}{\partial \mathscr{E}_{\rm kep}} \frac{\partial \mathbf{X}_{\rm kep}}{\partial \mathscr{E}_{\rm kep}}, \tag{100}$$

with

$$\frac{\partial \dot{\mathbf{r}}_{(k)}}{\partial \mathscr{E}_{\rm kep}} = \frac{\partial \phi_{1(k+3)}}{\partial \mathscr{E}_{\rm kep}}, \qquad \frac{\partial^2 \dot{\mathbf{r}}_{(k)}}{\partial \mathscr{E}^2_{\rm kep}} = \frac{\partial^2 \phi_{1(k+3)}}{\partial \mathscr{E}^2_{\rm kep}}, \tag{101}$$

Table 1 Keplerian elements at epoch 54127.1553819 MJD for object 1 and 54127.2991319 MJD for object 2

Obj.	a	e	I	Ω	ω	ℓ
1	7818.10	0.0658	65.81	213.92	356.70	202.25
2	7396.00	0.0341	26.88	255.49	357.13	198.67

The values of a, e, I are exact, the others are approximated. Distances are expressed in km, angles in degrees

Table 2 Standard deviation (rms) of the errors added to the radar tracks

	α, δ (°)	ρ (m)
Case 1	0.20	1
Case 2	0.20	10
Case 3	0.15	1
Case 4	0.15	10

and

$$\frac{\partial \mathbf{X}_{\text{kep}}}{\partial \mathscr{E}_{\text{kep}}} = \begin{bmatrix} O_3 & O_3 \\ \frac{\partial(\dot{\Omega},\dot{\omega},\dot{\ell})}{\partial(a,e,I)} & O_3 \end{bmatrix}. \tag{102}$$

The expressions of

$$\frac{\partial \phi_1}{\partial \mathscr{E}_{\text{kep}}}, \quad \frac{\partial^2 \phi_1}{\partial \mathscr{E}_{\text{kep}}^2}, \quad \frac{\partial \Phi^{-1}}{\partial \mathscr{E}_{\text{att}}^*}, \quad \frac{\partial \mathbf{X}_{\text{kep}}}{\partial \mathscr{E}_{\text{kep}}}$$

are reported in "Appendices A, B, C".

8 Numerical tests

We show some numerical tests with two simulated objects whose orbital elements at some epoch are defined in Table 1. For the selected orbits, the perturbation due to the J_2 is dominant if we assume a small area-to-mass ratio of the two objects (see Montenbruck and Gill 2000, Figure 3.1). Moreover, the J_2 effect will be stronger for object 2 because of the smaller values of the inclination and semi-major axis.

A two-body propagation with the J_2 effect (Eq. 23) is used to generate pairs of radar tracks at epochs $\tilde{t}_1, \tilde{t}_2$ of four observations each taken at time intervals of 10 s; see (1). Then, we add to ρ, α, δ a Gaussian error with zero mean and the standard deviation (rms) shown in Table 2. In Cases 1, 3, a small error is added to ρ,[3] while in Cases 2, 4 a significant noise affects both the angles and the range. For each object, we consider two pairs of radar tracks, separated by a different number of revolutions k. The interpolated data that we get after adding the noise to the simulated observations are given in Tables 3, 4 for object 1 and Tables 5, 6 for object 2. Note that also the values of $\dot{\alpha}, \dot{\delta}$ are shown because they are needed to initialize the unknown variables ξ, ζ.

Tables 7 and 8 report the absolute errors in each orbital element of objects 1, 2 at epoch $\tilde{t}_1$. For both objects, the new method, here referred to as IA-J_2, is able to correct the errors in α, δ and to recover the Keplerian elements of the known orbits with a satisfactory level

[3] Note that even if the rms of ρ was 0, the interpolated values of $\rho, \dot{\rho}$ at time $\tilde{t}_1$ would not be exact in general.

Table 3 Data interpolated from two radar tracks of object 1 at epochs $\bar{t}_1 = 54127.1553820$ MJD and $\bar{t}_2 = 54127.5824653$ MJD, using two different noise levels of Table 2

Epoch	Case	$\bar{\alpha}$ (°)	$\bar{\delta}$ (°)	$\dot{\alpha}$ (°/s)	$\dot{\delta}$ (°/s)	ρ (km)	$\dot{\rho}$ (km/s)
Object 1, $k = 5$							
$\bar{t}_1$	1	40.71190	− 4.34972	0.06933	− 0.17402	1965.89061	− 1.26651
	2	40.71190	− 4.34972	0.06933	− 0.17402	1965.88651	− 1.26557
$\bar{t}_2$	1	243.02897	− 79.04074	− 0.02136	0.16045	1875.99129	− 4.84869
	2	243.02897	− 79.04074	− 0.02136	0.16045	1876.00141	− 4.85139

The number of revolutions k, as defined in Eq. (62), is also reported

Table 4 Same as in Table 3 for two radar tracks at $\bar{t}_1 = 54127.5824653$ MJD and $\bar{t}_2 = 54128.6241320$ MJD

Epoch	Case	$\bar{\alpha}$ (°)	$\bar{\delta}$ (°)	$\dot{\alpha}$ (°/s)	$\dot{\delta}$ (°/s)	ρ (km)	$\dot{\rho}$ (km/s)
Object 1, $k = 13$							
$\bar{t}_1$	3	242.95755	− 79.11215	− 0.01356	0.16825	1875.98971	− 4.84829
	4	242.95755	− 79.11215	− 0.01356	0.16825	1875.98562	− 4.84735
$\bar{t}_2$	3	204.34455	53.03103	0.11860	0.10845	2061.14383	5.59005
	4	204.34455	53.03103	0.11860	0.10845	2061.15395	5.58735

Table 5 Data interpolated from two radar tracks of object 2 at epochs $\bar{t}_1 = 54127.2991320$ MJD and $\bar{t}_2 = 54127.3828126$ MJD, using two different noise levels of Table 2

Epoch	Case	$\bar{\alpha}$ (°)	$\bar{\delta}$ (°)	$\dot{\alpha}$ (°/s)	$\dot{\delta}$ (°/s)	ρ (km)	$\dot{\rho}$ (km/s)
Object 2, $k = 1$							
$\bar{t}_1$	1	72.88079	34.57579	0.20066	− 0.04293	1942.23386	− 3.40688
	2	72.88079	34.57579	0.20066	− 0.04293	1942.22977	− 3.40593
$\bar{t}_2$	1	193.80043	− 31.71774	0.13680	0.03447	2057.69443	5.00361
	2	193.80043	− 31.71774	0.13680	0.03447	2057.70455	5.00091

The number of revolutions k, as defined in Eq. (62), is also reported

Table 6 Same as in Table 5 for two radar tracks at $\bar{t}_1 = 54127.6906251$ MJD and $\bar{t}_2 = 54128.3300348$ MJD

Epoch	Case	$\bar{\alpha}$ (°)	$\bar{\delta}$ (°)	$\dot{\alpha}$ (°/s)	$\dot{\delta}$ (°/s)	ρ (km)	$\dot{\rho}$ (km/s)
Object 2, $k = 8$							
$\bar{t}_1$	3	162.41862	− 0.70695	0.12744	0.07974	1914.59715	− 5.09806
	4	162.41862	− 0.70695	0.12744	0.07974	1914.59305	− 5.09712
$\bar{t}_2$	3	169.53245	− 20.90422	0.14196	− 0.01396	2013.14698	4.73488
	4	169.53245	− 20.90422	0.14196	− 0.01396	2013.15710	4.73218

of accuracy. Note that the performance of the new method is only slightly affected by the increase of the noise level in ρ (Cases 2, 4).

We have also compared IA-J_2 to the method IAQ proposed in Gronchi et al. (2015b) which does not take into account the effect of the J_2 term of the geopotential. The advantage of IA-J_2 over IAQ becomes evident when the time interval between two radar tracks increases.

Table 7 Difference (in absolute value) between the computed and true orbital elements of objects 1, 2 at epoch $\tilde{t}_1$ for the interpolated data of Tables 3 and 5

	Object 1, $k = 5$		Object 2, $k = 1$		Case
	IAQ	IA-J_2	IAQ	IA-J_2	
δa	6.1476	1.1441	5.0957	1.7662	1
	171.4962	1.8259	10.3163	1.3280	2
δe	1.79×10^{-4}	4.43×10^{-5}	4.57×10^{-4}	4.30×10^{-4}	1
	1.48×10^{-2}	7.21×10^{-5}	2.04×10^{-3}	2.75×10^{-4}	2
δI	1.8416	0.4283	0.9966	0.3384	1
	0.8353	0.7366	0.1597	0.2694	2
$\delta\Omega$	0.0677	0.2408	1.1446	0.4020	1
	3.1663	0.4204	0.1827	0.3051	2
$\delta\omega$	3.7614	1.1999	0.8886	1.6806	1
	6.2622	1.8956	6.1047	1.3220	2
$\delta\ell$	4.3016	1.2948	0.0334	1.4552	1
	7.9420	2.0320	6.8222	1.1558	2

The new method is compared to the method IAQ proposed in Gronchi et al. (2015b). Distances are expressed in km, angles in degrees

Table 8 Same as in Table 7 for the interpolated data of Tables 4 and 6

	Object 1, $k = 13$		Object 2, $k = 8$	Case
	IAQ	IA-J_2	IA-J_2	
δa	502.4785	0.0105	0.1615	3
	502.4096	0.0116	0.1378	4
δe	4.32×10^{-3}	7.08×10^{-5}	2.00×10^{-4}	3
	4.76×10^{-3}	1.44×10^{-4}	1.50×10^{-4}	4
δI	6.2022	0.0977	0.9485	3
	6.2071	0.0830	0.6724	4
$\delta\Omega$	5.1509	0.0469	0.5746	3
	5.1487	0.0454	0.3900	4
$\delta\omega$	129.2975	0.0203	4.7886	3
	129.3858	0.0388	3.5505	4
$\delta\ell$	239.9665	0.0124	4.2105	3
	239.8206	0.0095	3.1483	4

The method IAQ does not work for object 2 when we take two radar tracks separated by 8 revolutions

Table 8 shows that by taking two radar tracks of object 1 separated by 13 revolutions, the method IAQ does not find a good orbit, while IA-J_2 is able to determine very accurate values of the orbital elements. Also, IAQ does not work with two radar tracks of object 2 separated by 8 revolutions, while IA-J_2 keeps the errors small. Finally, the corrections to the angles α, δ computed by the method IA-J_2 are shown in Tables 9 and 10.

Table 9 Infinitesimal angles (°) found by the proposed method using the radar tracks of Tables 3 and 4 for object 1

	Case 1	Case 2	Case 3	Case 4
$\Delta\alpha_1$	− 1.31448	− 2.30805	0.25737	0.08057
$\Delta\delta_1$	− 0.37447	− 0.69638	0.08058	0.07575
$\Delta\alpha_2$	0.71856	1.23111	− 0.23547	− 0.24423
$\Delta\delta_2$	0.32881	0.58535	− 0.02666	− 0.04653

Table 10 Infinitesimal angles (°) found by the proposed method using the radar tracks of Tables 5 and 6 for object 2

	Case 1	Case 2	Case 3	Case 4
$\Delta\alpha_1$	0.42261	0.31791	− 0.01612	− 0.00648
$\Delta\delta_1$	0.35088	0.26697	− 1.54546	− 1.12770
$\Delta\alpha_2$	0.30596	0.24228	0.03328	0.00800
$\Delta\delta_2$	− 0.82680	− 0.67820	− 3.45550	− 2.44161

9 Conclusions

We propose a new method to compute preliminary orbits of Earth satellites taking into account the Earth oblateness. The method attempts to link together two radar tracks, which may be separated by several revolutions. It consists in solving system (53) by a double-iterative scheme to determine the corrections of α, δ and the angular velocity. Numerical tests show that this IOD method works also in the presence of a significant noise level on the range and the angles. Future work will be to include the effect of the atmospheric drag and perform large-scale tests on LEO objects with real observations.

Acknowledgements This work is partially supported by the Marie Curie Initial Training Network Stardust, FP7-PEOPLE-2012-ITN, Grant Agreement 317185.

Compliance with ethical standards

Conflict of interest The authors declare that they have no conflict of interest.

Appendix A

The Jacobian matrix of the Cartesian coordinates $\mathscr{E}_{\text{car}}$ with respect to the Keplerian elements $\mathscr{E}_{\text{kep}}$ (see Eqs. 14, 15) can be obtained from Table 2 in Broucke (1970) by setting $t = 0$ in the expressions of $\frac{\partial\phi_1}{\partial a}$ and noting that $\frac{\partial\phi_1}{\partial\ell} = \frac{\partial\phi_1}{\partial M_0}$, where M_0 denotes the mean anomaly at epoch in Broucke (1970).

Let us adopt here and in "Appendix B" the same notation explained in Section 7.3 to refer to the component of a vector and a map. The derivatives $\frac{\partial^2\phi_{1(i)}}{\partial\mathscr{E}_{\text{kep}}^2}$, $i = 4, 5, 6$, are given by:

$$\frac{\partial^2\phi_{1(i)}}{\partial\mathscr{E}_{\text{kep}}\partial a} = -\frac{1}{2a}\left(-\frac{3\dot{\mathbf{r}}_{(k)}}{2a}, \frac{\partial\phi_{1(i)}}{\partial e}, \frac{\partial\phi_{1(i)}}{\partial I}, \frac{\partial\phi_{1(i)}}{\partial\Omega}, \frac{\partial\phi_{1(i)}}{\partial\omega}, \frac{\partial\phi_{1(i)}}{\partial\ell}\right),$$

$$\frac{\partial}{\partial(a,e,\ell)}\frac{\partial\phi_{1(i)}}{\partial e} = \frac{\partial\dot{L}}{\partial(a,e,\ell)}\mathbf{P}_{(k)} + \frac{\partial\dot{M}}{\partial(a,e,\ell)}\mathbf{Q}_{(k)},$$

$$\frac{\partial}{\partial(I,\Omega,\omega)}\frac{\partial\phi_{1,(i)}}{\partial e}=\dot{L}\frac{\partial\mathbf{P}_{(k)}}{\partial(I,\Omega,\omega)}+\dot{M}\frac{\partial\mathbf{Q}_{(k)}}{\partial(I,\Omega,\omega)},$$
$$\frac{\partial}{\partial(a,e,\ell)}\frac{\partial\phi_{1(i)}}{\partial I}=\Big(\frac{\partial\dot{X}}{\partial(a,e,\ell)}\sin\omega+\frac{\partial\dot{Y}}{\partial(a,e,\ell)}\cos\omega\Big)\mathbf{R}_{(k)},$$
$$\frac{\partial}{\partial(I,\Omega)}\frac{\partial\phi_{1(i)}}{\partial I}=(\dot{X}\sin\omega+\dot{Y}\cos\omega)\frac{\partial\mathbf{R}_{(k)}}{\partial(I,\Omega)},$$
$$\frac{\partial^2\phi_{1(i)}}{\partial\omega\partial I}=(\dot{X}\cos\omega-\dot{Y}\sin\omega)\mathbf{R}_{(k)},$$
$$\frac{\partial}{\partial\mathscr{E}_{\rm kep}}\frac{\partial\phi_{1(4)}}{\partial\Omega}=-\frac{\partial\phi_{1(5)}}{\partial\mathscr{E}_{\rm kep}},$$
$$\frac{\partial}{\partial\mathscr{E}_{\rm kep}}\frac{\partial\phi_{1(5)}}{\partial\Omega}=\frac{\partial\phi_{1(4)}}{\partial\mathscr{E}_{\rm kep}},$$
$$\frac{\partial}{\partial\mathscr{E}_{\rm kep}}\frac{\partial\phi_{1(6)}}{\partial\Omega}=0,$$
$$\frac{\partial}{\partial(a,e,\ell)}\frac{\partial\phi_{1(i)}}{\partial\omega}=\frac{\partial\dot{X}}{\partial(a,e,\ell)}\mathbf{Q}_{(k)}-\frac{\partial\dot{Y}}{\partial(a,e,\ell)}\mathbf{P}_{(k)},$$
$$\frac{\partial}{\partial(I,\Omega,\omega)}\frac{\partial\phi_{1(i)}}{\partial\omega}=\dot{X}\frac{\partial\mathbf{Q}_{(k)}}{\partial(I,\Omega,\omega)}-\dot{Y}\frac{\partial\mathbf{P}_{(k)}}{\partial(I,\Omega,\omega)},$$
$$\frac{\partial\phi^2_{1(i)}}{\partial a\partial\ell}=n\frac{a^2}{r^3}\Big(\frac{3}{2}\mathbf{r}_{(k)}-a\frac{\partial\phi_{1(k)}}{\partial a}\Big),$$
$$\frac{\partial}{\partial(e,\ell)}\frac{\partial\phi_{1(i)}}{\partial\ell}=n\frac{a^3}{r^3}\Big(3\frac{\mathbf{r}_{(k)}}{r}\frac{\partial r}{\partial(e,\ell)}-\frac{\partial\phi_{1(k)}}{\partial(e,\ell)}\Big),$$
$$\frac{\partial}{\partial(I,\Omega,\omega)}\frac{\partial\phi_{1(i)}}{\partial\ell}=-n\frac{a^3}{r^3}\frac{\partial\phi_{1(k)}}{\partial(I,\Omega,\omega)},$$

where $k=i-3$, and the quantities $\dot{X}$, $\dot{Y}$, $\dot{L}$, $\dot{M}$, $\mathbf{P}$, $\mathbf{Q}$, $\mathbf{R}$ are defined in Broucke (1970). We have

$$\frac{\partial\mathbf{P}}{\partial I}=(\mathbf{P}_3\sin\Omega,\,-\mathbf{P}_3\cos\Omega,\,\sin\omega\cos I)^{\rm T},$$
$$\frac{\partial\mathbf{P}}{\partial\Omega}=(-\mathbf{P}_2,\,\mathbf{P}_1,\,0)^{\rm T},$$
$$\frac{\partial\mathbf{P}}{\partial\omega}=\mathbf{Q},$$
$$\frac{\partial\mathbf{Q}}{\partial I}=(\mathbf{Q}_3\sin\Omega,\,-\mathbf{Q}_3\cos\Omega,\,\cos\omega\cos I)^{\rm T},$$
$$\frac{\partial\mathbf{Q}}{\partial\Omega}=(-\mathbf{Q}_2,\,\mathbf{Q}_1,\,0)^{\rm T},$$
$$\frac{\partial\mathbf{Q}}{\partial\omega}=-\mathbf{P},$$
$$\frac{\partial\mathbf{R}}{\partial I}=(\sin\Omega\cos I,\,-\cos\Omega\cos I,\,-\sin I)^{\rm T},$$
$$\frac{\partial\mathbf{R}}{\partial\Omega}=(\cos\Omega\sin I,\,\sin\Omega\sin I,\,0)^{\rm T},$$
$$\frac{\partial\mathbf{R}}{\partial\omega}=\mathbf{0},$$

and

$$\begin{aligned}
&\frac{\partial \dot{L}}{\partial a} = -\frac{\dot{L}}{2a}, \qquad \frac{\partial \dot{M}}{\partial a} = -\frac{\dot{M}}{2a},\\
&\frac{\partial \dot{L}}{\partial e} = n\frac{a^4}{r^4}(2r+a)\sin^3 E - \frac{3\dot{L}}{r}\frac{\partial r}{\partial e},\\
&\frac{\partial \dot{M}}{\partial e} = \dot{M}\Big(\frac{e}{1-e^2} - \frac{3}{r}\frac{\partial r}{\partial e}\Big)\\
&\qquad + \frac{n}{\sqrt{1-e^2}}\frac{a^4}{r^3}\Big[2e - 3\cos E + (2+\frac{a}{r})\cos^3 E + \frac{a}{r}(e-2\cos E)\Big],\\
&\frac{\partial \dot{L}}{\partial \ell} = n\frac{a^4}{r^4}\Big[2r\sin^2 E + (e - 2\cos E + e\cos^2 E)\Big(a\cos E - 3\frac{\partial r}{\partial \ell}\Big)\Big],\\
&\frac{\partial \dot{M}}{\partial \ell} = \frac{n}{\sqrt{1-e^2}}\frac{a^5}{r^4}\sin E\Big[e - 4\cos E + 3e\cos^2 E - \frac{3ae}{r}(e^2 - 1 - e\cos E\\
&\qquad + 2\cos^2 E - e\cos^3 E)\Big].
\end{aligned}$$

Finally, the derivatives of $\dot{X}$, $\dot{Y}$, r that appear in the previous expressions can be found in Broucke (1970, Table 1).

Appendix B

Let us introduce the coordinate change from $\mathscr{E}^*_{\rm att}$ to $\mathscr{E}_{\rm car}$ as the composite transformation

$$\psi = \phi_2^{-1} \circ \phi_3^{-1}.$$

Then, we have

$$\frac{\partial \Phi^{-1}}{\partial \mathscr{E}^*_{\rm att}} = \Big(\frac{\partial \phi_1}{\partial \mathscr{E}_{\rm kep}}\Big)^{-1}\frac{\partial \psi}{\partial \mathscr{E}^*_{\rm att}},$$

where $(k = 1, 2, 3)$

$$\begin{aligned}
&\frac{\partial \psi_{(k)}}{\partial \mathscr{E}^*_{\rm att}} = (\rho \mathbf{e}^{\alpha}_{(k)}\cos\delta,\ \rho\mathbf{e}^{\delta}_{(k)},\ 0,\ 0, \mathbf{e}^{\rho}_{(k)},\ 0)^{\rm T},\\
&\frac{\partial \psi_{(k+3)}}{\partial \mathscr{E}^*_{\rm att}} = (\xi \mathbf{e}^{\perp}_{(k)} + \mathbf{e}^{\alpha}_{(k)}(\dot{\rho}\cos\delta - \zeta\sin\delta), \dot{\rho}\mathbf{e}^{\delta}_{(k)} - \zeta\mathbf{e}^{\rho}_{(k)},\ \mathbf{e}^{\alpha}_{(k)},\ \mathbf{e}^{\delta}_{(k)},\ 0,\ \mathbf{e}^{\rho}_{(k)})^{\rm T},
\end{aligned}$$

with

$$\mathbf{e}^{\perp} = (-\cos\alpha,\ -\sin\alpha,\ 0)^{\rm T}.$$

Appendix C

We can write

$$\frac{\partial(\mathbf{X}_{\rm kep}\circ\Phi^{-1})}{\partial \mathscr{E}^*_{\rm att}} = \frac{\partial \mathbf{X}_{\rm kep}}{\partial \mathscr{E}_{\rm kep}}\frac{\partial \Phi^{-1}}{\partial \mathscr{E}^*_{\rm att}},$$

where

$$\frac{\partial\dot{\Omega}}{\partial a} = -\frac{3}{2}J_2\frac{R_\oplus^2}{p^2}\cos I\Big(\frac{\partial\tilde{n}}{\partial a} - \frac{2\tilde{n}}{a}\Big),$$
$$\frac{\partial\dot{\Omega}}{\partial e} = -\frac{3}{2}J_2\frac{R_\oplus^2}{p^2}\cos I\Big(\frac{\partial\tilde{n}}{\partial e} + \frac{4\tilde{n}e}{1-e^2}\Big),$$
$$\frac{\partial\dot{\Omega}}{\partial I} = -\frac{3}{2}J_2\frac{R_\oplus^2}{p^2}\Big(\frac{\partial\tilde{n}}{\partial I}\cos I - \tilde{n}\sin I\Big),$$
$$\frac{\partial\dot{\omega}}{\partial a} = \frac{3}{4}J_2\frac{R_\oplus^2}{p^2}(4-5\sin^2 I)\Big(\frac{\partial\tilde{n}}{\partial a} - \frac{2\tilde{n}}{a}\Big),$$
$$\frac{\partial\dot{\omega}}{\partial e} = \frac{3}{4}J_2\frac{R_\oplus^2}{p^2}(4-5\sin^2 I)\Big(\frac{\partial\tilde{n}}{\partial e} + \frac{4\tilde{n}e}{1-e^2}\Big),$$
$$\frac{\partial\dot{\omega}}{\partial I} = \frac{3}{4}J_2\frac{R_\oplus^2}{p^2}\Big[\frac{\partial\tilde{n}}{\partial I}(4-5\sin^2 I) - 5\sin(2I)\tilde{n}\Big],$$
$$\frac{\partial\tilde{n}}{\partial a} = \frac{\partial n}{\partial a} - \frac{21}{4}J_2\frac{R_\oplus^2}{p^2}\frac{n}{a}\Big(1-\frac{3}{2}\sin^2 I\Big)\sqrt{1-e^2},$$
$$\frac{\partial\tilde{n}}{\partial e} = \frac{9}{2}J_2\frac{R_\oplus^2}{p^2}\Big(1-\frac{3}{2}\sin^2 I\Big)\frac{ne}{\sqrt{1-e^2}},$$
$$\frac{\partial\tilde{n}}{\partial I} = -\frac{9}{2}J_2\frac{R_\oplus^2}{p^2}n\sin I\cos I\sqrt{1-e^2}.$$

References

Broucke, R.A.: On the Matrizant of the Two-Body Problem. Astron. Astrophys. **6**, 173–182 (1970)

Celletti, A., Galeş, C.: Dynamics of Resonances and Equilibria of Low Earth Objects. SIAM J. Appl. Dyn. Syst. **17**(1), 203–235 (2018)

Celletti, A., Negrini, P.: Non-integrability of the problem of motion around an oblate planet. Celest. Mech. Dyn. Astron. **61**(3), 253–260 (1981)

Daquin, J., Rosengren, A.J., Alessi, E.M., Deleflie, F., Valsecchi, G.B., Rossi, A.: The dynamical structure of the MEO region: long-term stability, chaos, and transport. Celest. Mech. Dyn. Astron. **124**(4), 335–366 (2016)

Farnocchia, D., Tommei, G., Milani, A., Rossi, A.: Innovative methods of correlation and orbit determination for space debris. Celest. Mech. Dyn. Astron. **107**(1–2), 169–185 (2010)

Gallego, G., Yezzi, A.: A Compact Formula for the Derivative of a 3-D Rotation in Exponential Coordinates. J. Math. Imaging Vis. **51**(3), 378–384 (2015)

Gronchi, G.F., Baù, G., Marò, S.: Orbit determination with the two-body integrals. III. Celest. Mech. Dyn. Astron. **123**(2), 105–122 (2015a)

Gronchi, G.F., Dimare, L., Bracali Cioci, D., Ma, H.: On the computation of preliminary orbits for Earth satellites with radar observations. Mon. Not. R. Astron. Soc. **451**(2), 1883–1891 (2015b)

Milani, A., Gronchi, G.F.: Theory of Orbit Determination. Cambridge University Press, New York (2010)

Montenbruck, O., Gill, E.: Satellite Orbits—Models, Methods and Applications, 1st edn. Springer, The Netherlands (2000)

Rosengren, A.J., Scheeres, D.J.: Long-term dynamics of high area-to-mass ratio objects in high-Earth orbit. Adv. Space Res. **52**(8), 1545–1560 (2013)

Roy, A.E.: Orbital Motion, 4th edn. CRC Press, Boca Raton (2004)

Siminski, J.A., Montenbruck, O., Fiedler, H., Schildknecht, T.: Short-arc tracklet association for geostationary objects. Adv. Space Res. **53**(8), 1184–1194 (2014)

Taff, L.G., Hall, D.L.: The use of angles and angular rates. I: Initial Orbit Determination. Celest. Mech. Dyn. Astron. **16**(4), 481–488 (1977)

Vananti, A., Schildknecht, T., Siminski, J.A., Jilete, B., Flohrer, T.: Tracklet–tracklet correlation method for radar and angle observations. In: Flohrer, T., Schmitz, F. (eds.) Proceedings of the 7th European Conference on Space Debris, Darmstadt, Germany, 18–21 April 2017, ESA Space Debris Office (2017)